Overview of the Early Campaign Diagnostics for the SPARC Tokamak

M.L. Reinke[1a] I. Abramovic[1], A. Albert[1], K. Asai[1], J. Ball[2], J. Batko[1], J. Brettingen[1], D. Brunner[1], M. Cario[1], J. Carmichael[1], C. Chrobak[1], A. Creely[1], D. Cykman[1], M. Dalla Rosa[3], E. Dubas[1], C. Downey[1], A. Ferrera[1], J. Frenje[2], E. Fox-Widdows[1], R. Gocht[1], G. Gorini[3], R. Granetz[2], M. Greenwald[2], A. Grieve[1], M. Hanson[1], J. Hawke[1], T. Henderson[1], S. Hicks[1], J. Hillesheim[1], A. Hoffmann[1], I. Holmes[1], N. Howard[2], A. Hubbard[2], J.W. Hughes[2], J. Ilagan[1], J. Irby[2], M. Jean[1], G. Kaur[1], R. Kennedy[1], E. Kowalski[1], A.Q Kuang[1], R. Kulchy[1], M. LaCapra[1], C. Lafleur[1], M. Lagieski[1], R, Li[1], Y. Lin[2], T. Looby[1], R. Zubieta Lubo[1], S. Mackie[2], E. Marmar[2], S. McKanas[1], A. Moncada[1], R. Mumgaard[1], C.E. Myers[1], V. Nikolaeva[1], M. Nocente[3], S. Normile[2], C. Novoa[1], S. Ouellet[1], E. Panontin[2], C. Paz-Soldan[4], J. Pentecost[1], C. Perks[2], M. Petruzzo[3], M. Quinn[1], J. Raimond[1], P. Raj[1], M. Rebai[5], V. Riccardo[1], D. Rigamonti[5], J.E. Rice[2], A. Rosenthal[1], M. Safabakhsh[1], A. Saltos[1], J. Shanahan[1], M. Silva Sa[1], I. Song[1], J. Souza[1], B. Stein-Lubrano[2], I.G. Stewart[4], R. Sweeney[1], M. Tardocchi[5], A. Tinguely[2], D. Vezinet[1], X. Wang[2], J. Witham[1]

[1]*Commonwealth Fusion Systems, Devens, MA 01434, USA*
[2]*Plasma Science and Fusion Center, Massachusetts Institute of Technology, Cambridge, Massachusetts 02139, USA*
[3]*Department of Physics, University of Milano-Bicocca, Milan 20126, Italy*
[4]*Department of Applied Physics and Applied Mathematics, Columbia University, New York, NY, 10027, USA*
[5]*Institute for Plasma Science and Technology, National Research Council, Milan 20125, Italy*

(Presented XXXXX; received XXXXX; accepted XXXXX; published online XXXXX)

The SPARC tokamak is a high-field, B_{t0} ~ 12 T, medium sized, R_0=1.85 m, tokamak that is presently under construction in Devens, MA, led by Commonwealth Fusion Systems. It will be used to de-risk the high-field tokamak path to a fusion power plant and demonstrate the commercial viability of fusion energy. SPARC's first campaign plan is to achieve Q_{fus} > 1 using an ICRF-heated, < 10 MW, high current, I_p ~ 8.5 MA, L-mode fueled by D-T gas injection, and its second campaign will investigate H-mode operations in D-D. To facilitate plasma control and scientific learning, a targeted set of ~50 plasma diagnostics are being designed and built for operation during these campaigns. While nearly all diagnostics are based on established techniques, the pace of deployment, relative to first plasma, and the harshness of the thermal, electromagnetic and radiation environment are unprecedented for medium-sized tokamaks. An overview of the SPARC diagnostic set is given, providing context to further details communicated by the SPARC Team in companion publications that are system-specific. The systems engineering philosophy for SPARC diagnostics is outlined and the design and engineering verification process for components inside and outside the primary vacuum boundary are described. Diagnostics are mounted directly to the vacuum vessel as well as housed within a series of 8 midplane and 24 off-midplane, replaceable port plugs. With limited exceptions, signal conditioning, digitization electronics and cameras as well as lasers and microwave sources are localized to a series of 5 Diagnostic Lab spaces, totaling ~350 m^2, located >15 m from the center of the tokamak, on the other side of a 2.4 m concrete shielding wall. A series of 31 large-scale penetrations have been included in the SPARC Tokamak Hall to facilitate integration of early campaign diagnostics and to provide for upgradability.

I. INTRODUCTION

Commonwealth Fusion Systems (CFS) is a private company, founded in 2018, spun out of the MIT Plasma Science and Fusion Center. The mission of CFS is to fast-track the commercialization of fusion energy on a timescale that can mitigate climate change by innovating HTS-based, high-field magnets [1] and leveraging decades of scientific progress in understanding compact, high-field tokamaks [2]. The SPARC tokamak [3], is presently under construction in Devens, MA and will be used by scientists and engineers to answer key open questions to inform the design of the ARC power plant, early concepts of which are discussed in [4][5].

The motivation and need for plasma diagnostics in a commercial fusion R&D facility like SPARC is different than both a publicly funded facility, whose mission is to support a wide scientific user base, and a commercial power-plant, whose goal is to cost-effectively generate electricity. Plasma diagnostics are needed for real-time control as well as to make the inter-shot observations necessary to advance a scientific mission. As the focus shifts from a user facility to a power plant, what evolves is the ratio of diagnostics used to satisfy each of these needs.

[a)]Author to whom correspondence should be addressed: mreinke@cfs.energy.

SPARC is positioned in the middle of that evolution, with nearly all diagnostic systems having some role in real-time or plant-level control while also being leveraged to close plasma physics gaps. Some of the design decisions and approaches are inherent to its one-off, R&D role and, as such, may not make sense for neither a user facility nor a power plant.

Construction of the SPARC facility is led by CFS using funding provided by private investment, but the SPARC Team is multi-institutional, with, at present, contributions from close to 1000 people from over 20 institutions. The fast development timeline and limited resources of the SPARC project created a need to use demonstrated, high-TRL approaches to measure the plasma. Our approach leverages private-public partnerships, building a SPARC Diagnostics Team that combines people with deep fusion community heritage with those with experience outside of fusion that add a diverse set of engineering, design, supply-chain, manufacturing and assembly skill sets. While specific sub-components and materials require innovation and prototyping, the basic diagnostic techniques used on SPARC have been repeatedly demonstrated on previous tokamaks. In contrast to large bore, HTS magnets, which required new test stands to demonstrate [6], and for CFS to build a dedicated factory to fabricate them, SPARC diagnostic proof-of-concepts and integrated tests occurred over decades of government-sponsored research on fusion facilities around the world [7].

The need for another step-change improvement in plasma diagnostics to support real-time control of ARC is acknowledged, and has been discussed in scoping studies for devices like DEMO [8]. It is not a mission of SPARC's diagnostics to demonstrate the specific diagnostic technology that enables ARC operation. Instead, it is to identify the requirements that bound a minimum viable measurement set for a power plant. The scope of this manuscript is focused on the diagnostics that the SPARC Diagnostic Team is designing and building for Campaign #1 and Campaign #2. The focus of Campaign #1 will be integrated commissioning in H_2, ^4He and D_2 plasmas, leading to a demonstration of high-current, D-T fueled, ICRF-heated L-mode plasma which is estimated to reach $Q_{fus} > 1$ [9]. Campaign #2 will focus on demonstrating enhanced confinement regimes in D-D. Starting in Campaign #3, the diagnostics will be used in high power D-T scenarios which aim to target $Q_{fus} \sim 11$. Many of the diagnostics are designed to operate over SPARC's full lifetime and need to be deployed and/or be commissioned within the first two Campaigns. The SPARC operational parameters of these two scenarios are outlined in Table 1.

A primary purpose of this manuscript is to communicate details of the planned SPARC plasma diagnostics to two audiences. The first is potential scientific users of SPARC,

TABLE I. SPARC parameters for the primary reference discharge (PRD) and first campaign $Q_{fus} > 1$ L-mode (Q1L). Both have $R_o = 1.85\ m$, $a = 0.57\ m$ and assume $n_D = n_T$

Parameter	Units	PRD	Q1L
Plasma Current, I_p	MA	8.7	8.5
Toroidal Field	T	12.2	12.2
Elongation, κ_a		1.75	1.70
Normalized Confinement		H_{98} ~1.0	H_{89} ~ 1.0
Magnetic Geometry		DN	SN
Δt Flattop	sec	10	4.0
τ_E	sec	0.77	0.56
Ohmic Power	MW	1.7	5.8
ICRF Heating	MW	11.1	2.8
Fusion Power	MW	140	9.5
$\langle T_e \rangle$	keV	7.3	5.8
$\langle n_e \rangle$	10^{20} m^{-3}	3.1	1.1
Z_{eff}		1.5	2.9
W_{pl}	MJ	22.3	5.8

where this document provides the top-level details of what measurements SPARC will have and why. Through references and future citations, this will act as an index to publications that have more granular details. The second audience is those interested in designing future diagnostics for SPARC. The details provided should allow rough, conceptual scoping as to whether a new diagnostic would be feasible and could be integrated into the SPARC facility. This manuscript is broken down into the following sections. In Section II, the major design constraints are outlined. A cross-section of the vacuum vessel, Tokamak Hall and Diagnostic Labs are given to highlight what limits diagnostics being integrated into the vessel and facility spaces. Section III summarizes the top-level performance and functional requirements that the diagnostic systems meet and shows how these are mapped to the specific instrument sub-systems, with details in Supplemental Material associated with this manuscript. Also presented is a schematic layout for how the limited spaces have been apportioned to the various diagnostics. Section IV and Section V outline the design philosophy, challenges and opportunities for future enhancement of in-vessel and port-

based diagnostics. Section VI expands on the capabilities and design within the Diagnostics Labs and Section VII provides a brief summary.

II. MAJOR DESIGN CONSTRAINTS

More details on the overall design of the SPARC tokamak can be found in [3], and Table 1 highlights some of the engineering and plasma parameters relevant for diagnostics. This section focuses on outlining major constraints that bound diagnostic design, many of which will be installed throughout the 13,000 pulse, 10-year lifetime of SPARC. At R=1.85 m, a = 0.57 m SPARC is the size of existing medium-sized, cryostat encapsulated tokamaks like KSTAR [10] that have superconducting coils. This size similarity enables the transfer of know-how and technology from proven diagnostics, where features are constrained by geometry. The key distinguishing characteristic of SPARC is the use of HTS magnets which allow the on-axis field to reach 12.2 T and currents up to 8.7 MA. Despite having HTS coils, SPARC is a pulsed device with a $\Delta t_{flat} \sim 10\ s$.

SPARC is built on a green-field site, and the basic sizing and layout of the facility was completed while the diagnostic systems were in early conceptual design. Most of the detailed design of the diagnostic systems has proceeded with these features as boundary conditions rather than trying to simultaneously optimize the two. This approach has facilitated the speed of deployment for SPARC without encountering significant restrictions. Figure I shows a recent photograph of the Tokmak Hall, along with a top-down schematic. No diagnostic equipment is shown, with the goal of this section to outline the large-scale interfaces that constrain instrument design.

The SPARC cryostat, R ~ 4.6 m sits in the center of the Tokamak Hall with the midplane at Z ~ 5.0 m above the floor and total heigh of ~9.2 m. Diagnostics interface in two key ways, through the 18 slots in the floor, interleaved with the CFS logo, and through 33 penetrations in the 2.4 m thick east wall. These are labeled in Figure II, along with the layout of 5 Diagnostic Labs which will house equipment that cannot survive high neutron fluxes, rates of 1e11 n/cm^2/s estimated in the Tokamak Hall for the 140 MW Primary Reference Discharge (PRD). Wired connections from sensors in the tokamak go into the basement and either proceed directly to the Diagnostic Labs through east/west running cable tray or sent to analog front-end electronics (integrators, trans-impedance amplifiers) and then routed to the Diagnostic Labs. Teal colored vertical and east/west cable tray distribute the signals to signal conditioning and digitization electronics in the two floors of the Diagnostic Labs. Cable runs of 30-40 m are within distances that have been shown to work on existing tokamaks.

Four of the Lab spaces are of similar size, 9.0 x 8.2 m, and will house equipment that uses 24 of the 1.22 x 1.22 m penetrations. The upper north (UN) and upper south (US) labs also have a 20 cm diameter circular penetration (NLOS, SLOS) that points to the core of the plasma. The ground-level, lower north (LN) and lower south (LS) are being used for equipment that benefit from having the shortest cable runs as well as equipment that may require more stable mounting surfaces. The central lab space is taller and narrower and was designed specifically with neutron and gamma imaging in mind. The 6 larger penetrations (NC1-NC6) are 1.22 x 2.13 m, along with vertically extended 0.61 m wide penetration for poloidal imaging (NC0). These penetrations have been roughly allocated to different measurement systems, shown in Figure II, with labels referencing system names in Table II. Most of the void space in the penetrations will be refilled with shielding, as they were designed to be oversized in order to allow for future optionality and upgradability. This toroidally non-uniform layout of the Diagnostic Labs relative to the tokamak creates a pattern of utilization for the port-plugs that is evident in their layout discussed in the next section.

Another key interfacing limit for the diagnostics is the size layout of the SPARC vacuum vessel (VV) and in-vessel components. This is highlighted in Figure III with sizing indicated to help orient readers. Section IV and Figure V provide further detail related to sub-divertor diagnostics. The nominal size, shape and features of the VV, including the port plug locations, was locked early in the SPARC design, driven by non-diagnostic interface constraints. SPARC is fully up/down symmetric and lacks any vertical ports, which constrains a number of typical diagnostic approaches as well as adds to sensor count. There are 18 midplane port (MP) openings and 16 upper off-midplane and 16 lower off-midplane port (OMP) openings, though not all are filled with removable port plugs. Of the ~5100 diagnostic electrical pins that exit the primary vacuum boundary, ~3100 do so at 24 dedicated feedthrough sub-assemblies located above (below) the upper (lower) off-midplane port plugs, as identified in Figure III. This allows off-midplane port plugs to be exchanged without disturbing in-vessel diagnostic cabling.

Cooling of the diagnostics is accomplished primarily by circulating room-temperature He gas between the two shells of the VV and using conduction to transfer heat to the VV. This circuit is also used for baking SPARC, which can go up to 350 degC. Liquid cooling of any kind was restricted by top-level requirements and circulating gas cooling to discrete diagnostic components was avoided by choice. Some heat rejection via radiation to the cryostat thermal shield can occur for large major radius portions of the port extensions. This limited cooling eases design and integration in-vessel, but results in the temperature of the VV, PFCs and diagnostic components ratcheting up over an

8-hr run day. This ratcheting increases for components with larger conduction paths to the VV surface. Estimates from global thermal modeling indicate a 4-hr inter-pulse cooldown is necessary for the PRD while a full power, full-length D-D plasma requires nominally 40 minutes. SPARC systems, including diagnostics, are designed to be able to support an inter-pulse time of 20 minutes in cases where injected or generated energy is limited. This facilitates fast learning early in SPARC's operation.

Ability to observe emission from the plasma is a key requirement for many diagnostics, which is moderated by the plasma facing components. The PFC contour is available on-line at [11]. Poloidally, between the two OMP's, the PFC contour is toroidally discontinuous, with SPARC having 18 rail-style limiters (OLIM). With limited exceptions away from high-heat flux zones, discussed in Section IV, the PFCs are then toroidally continuous everywhere else. Areas in the main-chamber where there are no PFCs may have an excellent view, but also are outside of the protection PFCs provide. Having 18 limiters results in relatively short toroidal connection lengths, < 1 m, between PFC surfaces. Parallel conduction competes with cross-field transport to reduce the radial scale length of the far-SOL and electron+ion heat flux to spaces between limiters. The charge-exchange and photon flux remains high for many plasma viewing diagnostic components if left unshielded. Ray tracing estimates using HEAT [12] show that the front of port plugs will see 10-15 kW/m^2 for every MW of radiated power from the core. This corresponds to a heat flash of 0.32-0.47 MJ/m^2/s$^{1/2}$ for every MJ of core stored energy if released over a 1 ms thermal quench timescales.

Surviving disruptions is a key challenge for diagnostic components inside the SPARC TF field. Survival is defined by the SPARC Structural Design Criteria (SDC) which draws from the ASME Boiler and Pressure Vessel Code and the TPX SDC [13]. For many metallic components, the criteria which limits the size of diagnostic components is to keep primary stresses below 2/3 of the yield stress, at temperature, to avoid plastic collapse. Components are additionally analyzed for local failure and fatigue. Transient, spatially varying volumetric force densities are calculated using an in-house workflow starting with ANSYS Workbench and Mechanical APDL scripting, Induced 3D currents are modeled in a $\Delta\phi = 20^o$ sector of the tokamak with cyclically coupled boundary conditions. The dynamics of the plasma are represented by 193 current filaments, with two different scenarios, a vertical displacement event (VDE) and major disruption (MD). In the VDE scenario, the vertical position drifts exponentially, moving 0.6 m over 120 ms. The plasma cross-section shrinks, keeping the total current fixed until the edge safety factor reaches unity at which the current decays. In a major disruption, the plasma current decays at its centered position in the vacuum chamber. Both scenarios decay the total current exponentially as $e^{-t\,[ms]/1.385}$, a rate of decay that is derived from the ITPA disruption database scaling [14]. That work compiled cross-machine current quench data, and SPARC has chosen a value of $\Delta t_{80-20} = 3.2\ ms$, based on assuming all SPARC disruptions will occur at $\Delta t_{80-20}/S > 2.0\ [ms/m^2]$. For context setting, this results in dB_z/dt at the outboard midplane, where $B_p = 2.8\ T$, to be more than 2000 T/s at the initiation of the current quench. The resulting eddy currents induced in the vacuum vessel, nearby in-vessel structures and diagnostic components combine to create Lorentz body forces in objects, where the large toroidal field of SPARC further contributes on top of the high dB_p/dt. These loads are used as inputs into ANSYS structural simulations to compute stresses and compare to allowables. Since materials (e.g. strength, resistivity) and physical scale are similar to other medium sized tokamaks, SPARC's increase in B_T at similar desired range of q_* results in forces within diagnostic components that grow nominally quadratically with toroidal field compared to devices such as KSTAR, EAST, AUG and DIII-D. Using XM-19 instead of 316 stainless steel is a common tool to increase margin to allowable, but generally SPARC diagnostic components end up reducing in size or increasing in fabrication complexity to include features for eddy current suppression. The ANSYS workflow also can account for halo currents, but in general this is not a design driver for diagnostics. In the Tokamak Hall, dead-load and seismic loads are the primary structural design concerns and are independent of SPARC's compact, high-field approach relative to other tokamaks. SPARC's high current operation does result in increased residual poloidal magnetic fields outside of the cryostat, roughly 500 G at approximately 10 m from the center of the tokamak, at the midplane, and still above 20 G at the far end of the Diagnostic Labs. This increases the variety of components that need magnetic shielding in comparison to other medium-sized tokamaks. Error field studies show that within the Tokamak Hall at roughly 6 m < R < 12 m, ~10 kg of high permeability material should not create a negative impact to SPARC. Outside of 12 m, error field considerations don't restrict the mass of magnetic shielding material.

Figure I. Layout and sizing of the SPARC Tokamak Hall and positioning of the Diagnostic Labs to the east of the cryostat.

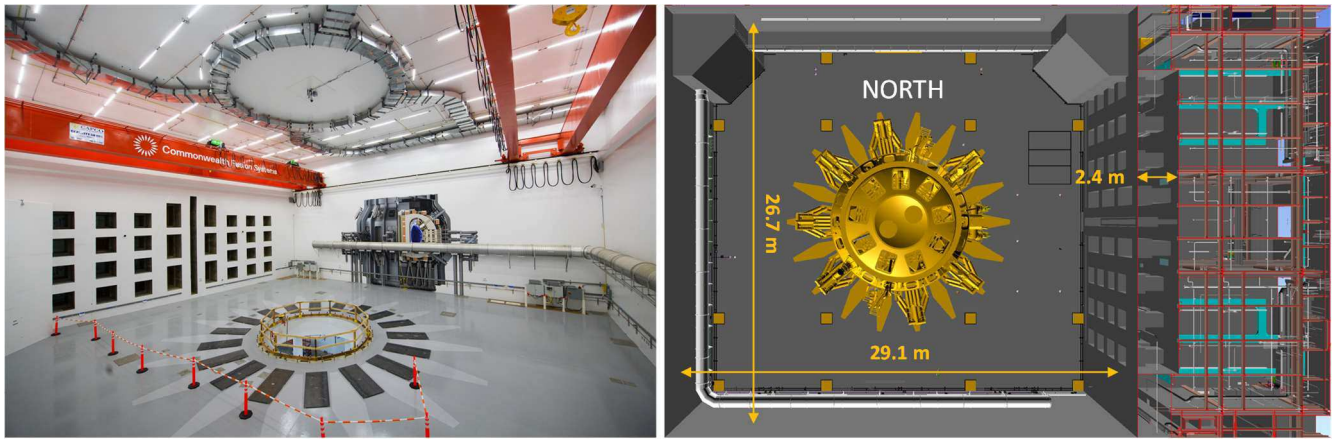

Figure II.. Layout and sizing of the Diagnostic Labs and early campaign utilization of the Diagnostic Hall Penetrations.

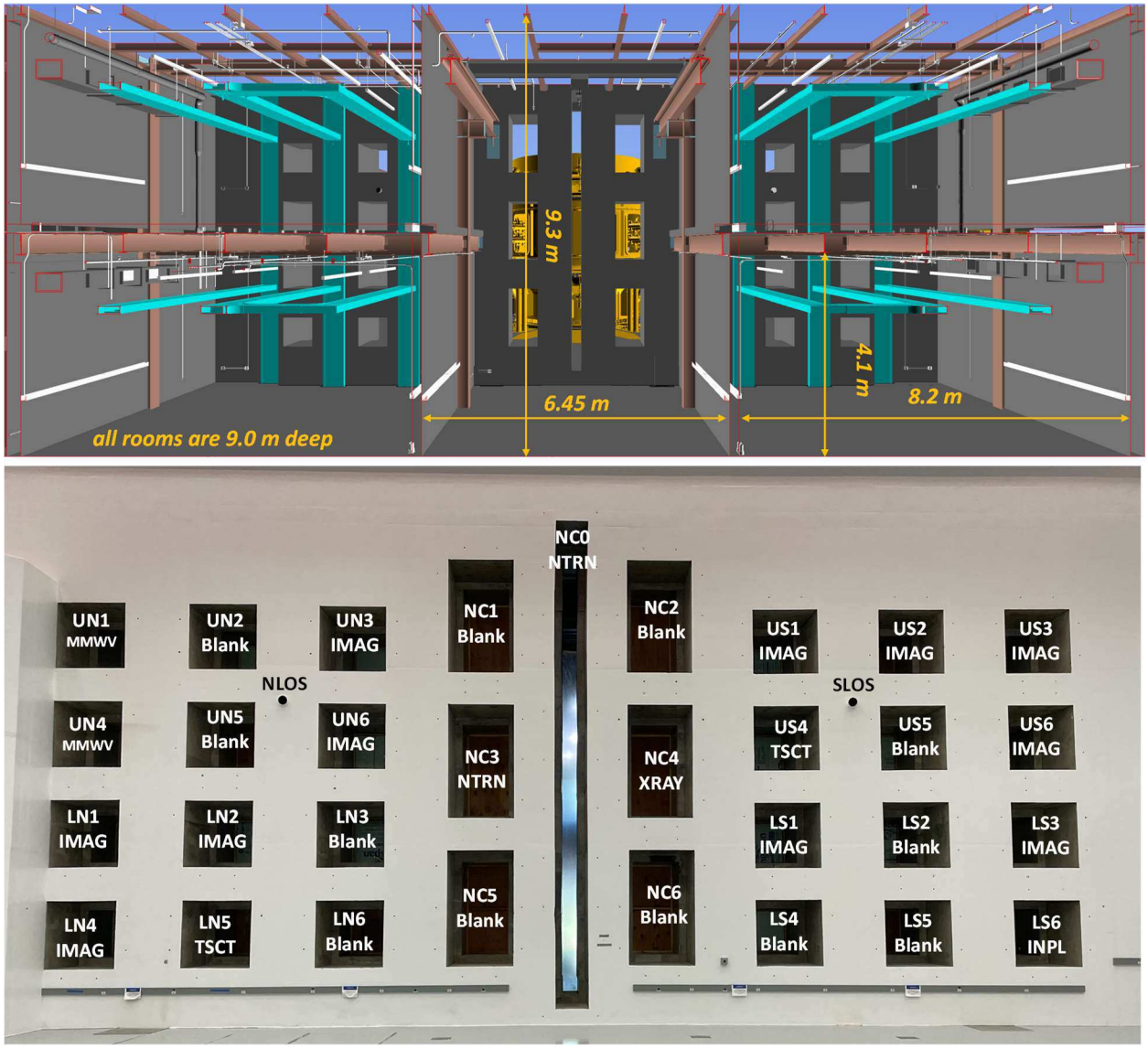

Figure III. Layout of SPARC vacuum vessel, port-extensions and major in-vessel components. The toroidal width of the port-extensions is 0.550 m and 0.375 m for the midplane and off-midplane, respectively.

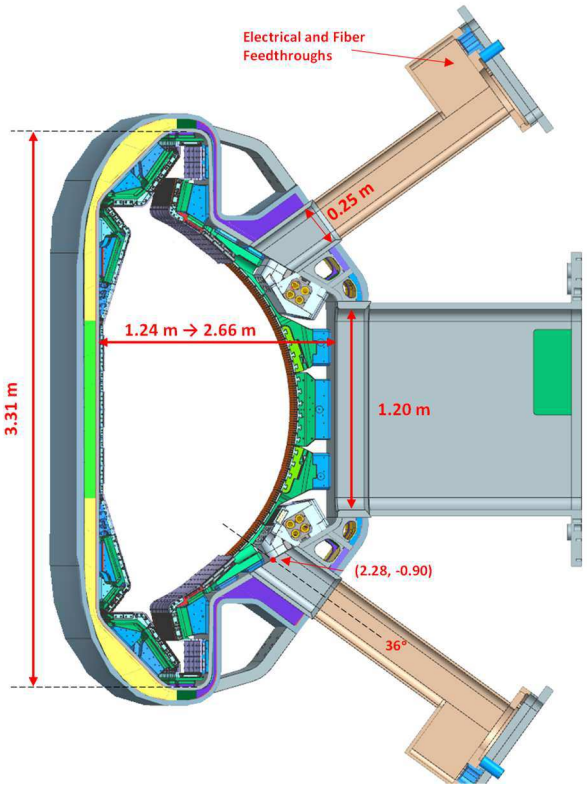

III. REQUIREMENTS AND SYSTEM LAYOUT

The scope of diagnostics for SPARC was outlined in mid-2020, in parallel with early engineering design of the larger structures and interfaces such as the vacuum vessel, PFCs, port-plugs and in-vessel coils. The top-level general requirements that bound the diagnostics were that they support tokamak operations in achieving the primary reference discharge and provide sufficient information to validate three primary missions: (a) demonstrate net fusion energy (Q_{fus} >1) and high gain (Q_{fus} ~ 11) (b) demonstrate divertor solutions for ARC design and (c) retire broader ARC physics risks. While all are more broadly defined in internal mission statements, there still was substantial room for interpretation of what precisely needed to be measured and why. To avoid a lengthy and costly concept of operations study early in the project, an approach was taken to leverage existing tokamak community knowledge and high-TRL demonstrations to identify the likely measurement classes that SPARC would inevitably need.

TABLE II. List of SPARC early campaign diagnostics

Diagnostic	Label	Early Campaign Scope
Magnetic Diagnostics	MAGX	flux loops, Ip Rogowski, Bx sensors, halo Rogowskis, high frequency Mirnovs
Interferometry and Polarimetry	INPL	single chord, two-color interferometer
Neutral Gas Diagnostics	NTGS	main-chamber + divertor neutral pressure and RGA
UV/Vis/IR Imaging	IMAG	multiple divertor, main-chamber and antenna imaging views
X-Ray Diagnostics	XRAY	hard X-ray, soft X-ray imaging, high- and low-resolution crystal spectroscopy
UV/Vis/IR Spectroscopy	SPEC	filterscopes, bremsstrahlung, H/D/T and ^{3}He/^{4}He isotope ratios, divertor and main chamber grating spectroscopy
Vacuum Spectroscopy	VCSP	core and divertor impurity spectroscopy
Bolometers	BOLO	divertor, core and disruption radiated power
Thermal Sensing	THRM	embedded thermocouples, FBGs, surface thermocouples in main-chamber + divertor
Neutron Diagnostics	NTRN	flux monitors, foil activation, poloidal imaging camera, core magnetic recoil spectrometer
Thomson Scattering	TSCT	low-resolution core profile measurement
Millimeter Wave Diagnostics	MMWV	electron cyclotron emission, edge scanning reflectometer
Langmuir Probes	LANG	divertor and main-chamber probes, current shunts
Displacement Sensing	DISP	vacuum vessel and coil displacement sensors
Strain Sensing	STRN	vacuum vessel strain sensors

This consisted of a down-selection from existing, proven techniques using surveys of complete diagnostic sets on ITER and existing devices, along with a prioritization relative to SPARC's mission goals. This resulted in 67 Level 3 (L3) instrumentation sub-systems in the SPARC product breakdown structure, where diagnostics (DIAG) is a Level 1 (L1) system. The goal of the SPARC Diagnostic Team is to pursue 45 of these for early campaigns. These are summarized in Table II at the Level 2 (L2) system level, which collects L3 sub-systems by technology and design challenge. Some diagnostics were excluded due the lack of supporting auxiliary systems, like neutral beams, and others excluded by risk avoidance, such as scanning probes and retractable material exposure stations. There are additional sub-systems being developed to facilitate cross-system measurements, such as electrical and fiber feedthroughs and radiation shielding, both of which aren't listed in Table 3. Additionally, the wider SPARC Team is developing more instrumentation for magnet and plant system control that is beyond the scope of this manuscript. The focus of the diagnostics are on making measurements of the plasma itself or sensing the impact of plasma-driven effects on the environment, such as thermal effects and electromagnetic forces from disruptions.

Even with measurement classes identified, further identification of function and purpose of the diagnostics was required to bound design. Quantitative requirements at the L1 system level were intentionally avoided to not create a situation where conservative physics assumptions would drive design churn. The list of sub-systems was further mapped into five Tiers to help prioritize schedule and need.

- Tier 1A: needed for first plasma and basic operation
- Tier 1B: needed for high power and high current operations
- Tier 2A: needed to achieve net fusion energy mission
- Tier 2B: needed to achieve the divertor mission
- Tier 2C: needed to achieve the ARC physics mission

General requirement statements were then developed by internal stakeholders and reviewed in early 2021, and have nominally remained unchanged since then. These typically take the form of 'DIAG shall measure or infer <some property/component> for the purposes of <some function/need>". For example 'DIAG shall measure or infer the temperature of the plasma facing components for the purpose of preventing damage' is a Tier 1B requirement and 'DIAG shall measure the D-T ratio for the purpose of

controlling fusion power' is a Tier 2A requirement. In total, there are 26 Tier 1A, 20 Tier 2B, 10 Tier 2A, 16 Tier 2B and 7 Tier 2C requirements. These requirements were then mapped, some non-exclusively, to the L2 system listed in Table II based on prior examples in tokamaks. The full list is shown in Supplemental Material. The process of conceptual and early preliminary design over 2021-2023 was to clarify these requirements into quantitative statements at the L2 or L3 system level that would then drive design. This facilitated early iterations where requirements were bound or adjusted by what was estimated to be feasible within the constraints of SPARC's engineering loads or resource limits. Being able to downgrade performance requirements or defer portions of a sub-system was key in maintaining early progress by avoiding 'desirements' (e.g. desires disguised as requirements) from research end-users driving substantial design churn or cost-escalation. This systems-engineering approach is somewhat non-standard for the ground-up development of a ~B$ science facility, but is generally reflective of how contemporary diagnostic deployment is the 'art of the possible' and consistent with the unique nature of the SPARC mission and team, highlighted in Section I.

In addition to time, material limits and cost, physical space is also a resource that impacts SPARC diagnostic design. SPARC being compact and high-field exacerbates this due to a smaller area to observe the plasma and a greater need for a fraction of that to be steel for structural support. The requirement to run in DT necessitates space be given to B_4C neutron shielding inside the primary vacuum boundary and to minimize approaches which require large, direct lines of sight. Figure III and IV show a schematic layout of how this space has been apportioned between diagnostics and other systems. Figure III shows the wire-ways and space reservations used to route cables from sensors mounted to the vacuum vessel to electrical and fiber feedthroughs. More details on the philosophy, challenges and enhancement opportunities are discussed in Section IV. The block diagram in Figure IV shows how the 18 midplane and 36 off-midplane port spaces are broken down between diagnostics, listed in Table II, and other systems. Note that ESRL and ECE are MMWV sub-systems and FOIL, NCAM and NSPC are NTRN sub-systems. More details are discussed in Section V.

The ability to upgrade portions of the diagnostic system over time, as well as some of the uncertainties in what SPARC might have encountered have resulted in a prioritization of resources that continuously impacts on-going design. Resources, especially time, is finite in a mission-driven project like SPARC. The priorities, in order, are for (a) the diagnostic system to be able to control plasmas needed in Campaign #1 while being resilient to a limited range of physics and technology risks, (b) make a reliable $Q_{fus} > 1$ measurement, (c) deploy redundancy for diagnostics that will be difficult to maintain after initial assembly and low-level activation, (d) deploy measurements needed in Campaign #2 that need to be commissioned using Campaign #1 plasmas and (e) be resilient to a broader range of Campaign #1 and Campaign #2 physics and technology risks.

Figure III. Layout of SPARC's wired, in-vessel diagnostics (INVD). Sub-system labels are outlined in Table II.

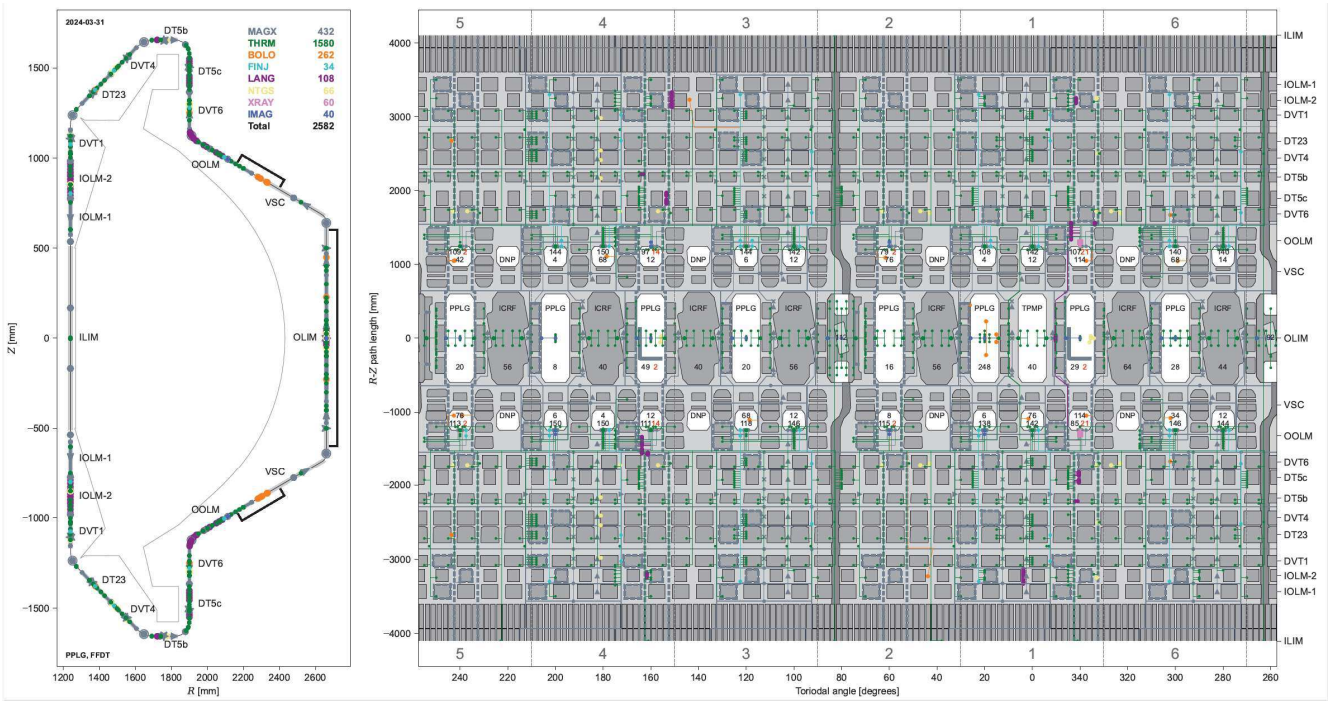

Figure IV. Layout of and use of SPARC's upper (UP) and lower (LP) off-midplane and midplane (MP) port plugs. View is from the inside of the vacuum vessel looking outward.

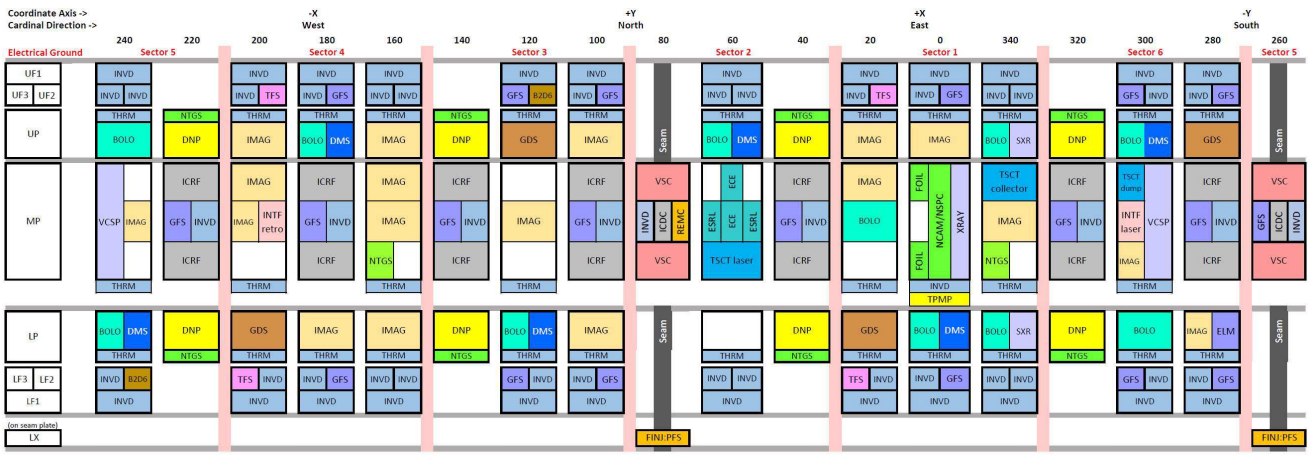

Index of non-diagnostic systems referenced in Figure 2. Table 2 provides an index for diagnostics systems.

Acronym	Description		Acronym	Description		Acronym	Description
INVD	collective reference for in-vessel diagnostics		GFS	gas fueling system (non-tritium)		ELM	ELM pellet pacing system
DNP	divertor neutral pumping		PFS	pellet fueling system		ICDC	ion cyclotron discharge cleaning antenna
B2D6	B_2D_6 injection for boronization		VSC	vertical stability coil feedthrough		GDS	glow discharge system
TFS	tritium fueling system		REMC	runway electron mitigation goal feedthrough		ICRF	4-strap ICRF antenna
DMS	massive gas injection based disruption mitigation system		TPMP	torus pumping system			

IV. IN-VESSEL DIAGNOSTIC DESIGN

For SPARC, in-vessel diagnostics refers to the class of sensors that are inside the vacuum vessel or exist between the vacuum vessel and cryostat, and have distinct challenges from diagnostics that are built into port-plugs, discussed in Section V. This section focuses on sensors on the plasma-side of the vacuum vessel from magnetics (MAGX) [15], neutral pressure sensors (NTGS) [16], bolometry (BOLO) [17], thermal sensors (THRM) [18] and Langmuir probes (LANG). Two Rogowski coils (MAGX), 44 thermocouples (THRM) as well as the entirety of the displacement (DISP) and strain (STRN) sub-systems are within the cryostat vacuum and outside of the scope of this manuscript.

Figure V provides a zoomed in view of Figure III, highlighting the in-vessel components that diagnostics need to design around. The PFC contour is displaced from the VV by discrete pedestals at 36 toroidal locations per poloidal sector, which creates a set of poloidally running 'highways'. A poloidally continuous gap of at least 3 cm wide is ensured from the inner limiter (ILIM) to the off-midplane port. At its narrowest, there is space only for MgO-based mineral insulated cables (MIC), fused silica fiber optic cables and gas fueling lines (FINJ). In zones behind the inner off-midplane limiter (IOLIM) and outer off-midplane limiter (OOLIM), which define the divertor throat, and the divertor tiles (T1 → T6) there is room for larger discrete sensors and even pinhole cameras (BOLO). As much as feasible, toroidally extended cable runs are avoided so that cables can exit the vacuum boundary at the same toroidal location. Poloidal flux measurements are made mostly using $\Delta\phi = 40^o$ partial flux loops, with only 8 full flux loops installed in locations of extended poloidal gaps between PFC support structures. The presence of the 4-turn vertical stability coils above and below the midplane port opening restricts routing in the region between the upper and lower OOLIM. Support structures for RF antennas and OLIM also restrict space for sensor mounting compared to other medium-sized and small tokamaks. Of the few in-vessel sensors that exist in this zone, many exit the primary vacuum boundary at ports that are not externally replaceable such as those that have ICRF antennas, those where in-vessel coil leads exit or the torus pumping port (see Figure III/IV). All MIC are hermetically sealed to limit out-gassing and low-voltage (1 A, 500 V), high-current (10 A, 500 V), high-voltage (1 A , 5000 V) as well as fiber-optic feedthroughs have a secondary space to mitigate the impact of leaks and tritium permeation. Pre-amplifier and back-end electronics for in-vessel sensors are grouped into 6 grounding zones, shown in Figure III, to avoid needing high channel-to-channel isolation from disruption induced voltages, as the full $V_{loop} > 1.0\ kV$ at the inner midplane.

Due to the high heat fluxes expected on SPARC divertor plasma facing components [19], multiple restrictions were put on interfacing diagnostics. In areas where pure-W is used (T1, T2, T4, T5b, T6 and OLIM) no top-surface holes are allowed, so there are no Langmuir probes or surface thermocouples (STC) anywhere that a primary strike point would be located for a single null (SN) or double null (DN) equilibrium. To avoid introducing stress concentrations in the pure-W, thermocouples are limited to the non-plasma facing side of the tungsten material and the interfacing steel mounting structures. Toroidal gaps between pure-W tiles were minimized and no dedicated gaps for plasma viewing diagnostics are accommodated as this would have created the need to locally enhance the fish-scale angle of the tiles and create a 'weak spot' in the divertor armor. Toroidally extended gaps are allowed where PFCs used tungsten heavy alloy (WHA) and were used to enable divertor views for BOLO. Dedicated gaps at four toroidal locations for divertor neutral pumping also allow for a view of the x-point target chamber which is formed by T5a, T5b, T5c and T5d, and the gap between T4 and T6. The vertically extended T5c surface is a WHA tile, which allows for STC and Langmuir probes to be installed, and this surface will be the landing point for strike points in an x-point target geometry [20].

Figure V. Layout of SPARC vacuum vessel, port-extensions and major in-vessel components. PFCs that use pure-W are shown in orange, while PFCs that use tungsten heavy alloy are shown in purple. Dedicated baffling (not shown) directs neutrals down the port-extension.

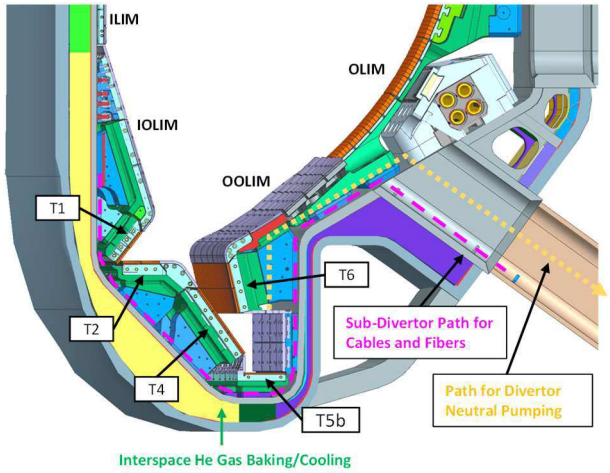

The main environmental challenges that in-vessel diagnostic sensors face are high temperatures from bake and electromagnetic loads from vertical displacement event disruptions. VV-mounted sensors are generally shielded from line-of-sight view of the plasma and nuclear heating is limited, 16-17 W/cm^3 in steel directly seeing the plasma and an order of magnitude lower behind PFCs, while also having the shortest path to the actively cooled surface. This makes qualifying sub-assemblies to survive bake, nominally set at 400 degC, as the critical thermal limit, while material

properties for surviving disruption are set at the 150 degC max operating temperature of the VV. Restrictions on materials for compatibility with tritium processing equipment and to limit activation also can also challenge design. No sulfide-based lubricants (e.g. MoS_2) or halogen containing materials are allowed. Despite their being ideal for high-temperature, high-strength applications there is no large-scale use of Ni-rich alloys in order to reduce activation. High-activation materials are limited to few kg-levels across diagnostics, used in small-scale components such as springs, pins or coatings.

The VDE scenario described in Section II is the main structural design driver for qualifying diagnostics sensors and cable tie-downs mounted to the vacuum vessel. These are a combination of loads generated by the eddy currents in the component itself due to local dB_p/dt, bending stresses imposed by the vacuum vessel for poloidally extended diagnostics and a moment about the normal of any sensor that is electrically connected to the vessel. In the latter, a fraction of the toroidally running currents in the vessel will follow a path radially in/out of a diagnostic component to produce this torque. For the same reason, poloidally running halo current may also run through the diagnostic, but this creates a force that compresses the sensor against the vessel and is not challenging to manage. The primary means that diagnostics use to react these loads is studs welded to the VV. Inertial loads from the vertical force are not meaningful due to the limited mass of sensors and the large eddy current loads.

The other main challenge for in-vessel diagnostics is designing and qualifying components assuming there is no in-vessel, sub-divertor maintenance. SPARC's mission and operational plan is designed to allow for a single in-vessel entry after Campaign #2. The extent of removal of in-vessel components is expected to be limited to only tiles and not removing their support plates which would allow access to the 'highways' and most of MAGX, NTGS, BOLO, THRM and LANG. This motivates including redundancy as well as using sensors with different potential failure modes to create defense in depth. While completion of the divertor mission is not planned to happen by the end of Campaign #2, many diagnostics that are required to achieve that mission need to be installed for first plasma.

V. PORT-BASED DIAGNOSTIC DESIGN

For SPARC, the port-based diagnostics refers to the class of sensors that are mounted to replaceable port-plugs. This restricts their ability to view the plasma but creates the possibility for upgrades. As shown in Figure IV, interferometry (INPL) [21], neutral pressure sensors (NTGS) [16], UV/visible/IR imaging (IMAG), X-ray spectroscopy (XRAY) [22], vacuum ultraviolet spectroscopy (VCSP) [23], bolometry (BOLO) [17], Thomson scattering (TSCT), and millimeter wave (MMWV) [24] all have major components occupying portions of port-plugs. Thermal sensing (THRM) [18] monitors the temperature of multiple port-plugs, and IMAG presently plans to include multiple fibers to be used to back-light for inter-shot inspection. CFS does not have a hot-cell at the SPARC facility for extraction, maintenance and re-installation of the first generation of port plugs. Features which are accessible from inside the assembled tokamak may be adjustable during the Campaign #2 entry if critical, but the baseline maintenance strategy for in-vacuum components is 'no maintenance'.

The primary functions of the port-plugs are to; (1) ensure the integrity of the primary vacuum boundary, (2) assist in reducing the neutron flux to allowable levels for the HTS coils and Tokamak Hall (3) and to provide a flexible, adaptable mounting structure for client systems like diagnostics. The sizing and internal components of a fully-shield port plug are shown in Figure VI for the midplane port plug and Figure VII for an off-midplane port plug. Major materials are B_4C (dark gray) and steel (light gray), with the plasma facing B_4C coated in W (green) to reduce the release of carbon via sputtering from C-X neutrals. The inner volume of the midplane port plug is filled via four (A→D) shielding shelves that are installed toroidally and four (A→D) septum trays that are installed radially. Diagnostic components are installed by removing areas of B_4C to create voids either for transmission of light, routing of cables or to install components such as mirrors. Diagnostic sub-assemblies can also mount directly to the side plates, the front of which is ~7 cm beyond the main limiter contour. No components can be mounted to the exterior of the plug to avoid clashing with the port extensions. The main design approach is for port plug clients to only require subtractive manufacturing from the baseline set of port-plug components, e.g. the removal of B_4C blocks and the addition of components that require unique hole patterns for assembly. This allows for the parallel fabrication of the main structural components to the point of a common set of blank parts while final diagnostic layout and design verification is completed. To avoid neutron streaming, direct lines of sight of the plasma from the air side of the port plug are not used except in key areas where they would compromise the function of the diagnostic, such as for core-viewing vacuum spectroscopy. MCNP modeling has shown that a single 90° dog-leg with length x2-x3 times the diameter of the void is sufficient. These are generally located within the shielding shelves. All diagnostics that need to transition light or cables through the port flange use standard Conflat-style sub-flanges ranging from DN40 to DN200, with a single instance of a DN250 planned for TSCT. All windows, fiber and electrical feedthroughs have an interspace that can be gas-backfilled and pumped to mitigate leaks and tritium permeation. These re-makable seal flanges are at the port-

Figure VI. Layout and sizing of a fully-shielded midplane port plug for SPARC. Diagnostic systems are integrated by making subtractive modifications to the baseline design by removing shielding blocks and creating tapped holes and voids for mounting components and creating lines of sight.

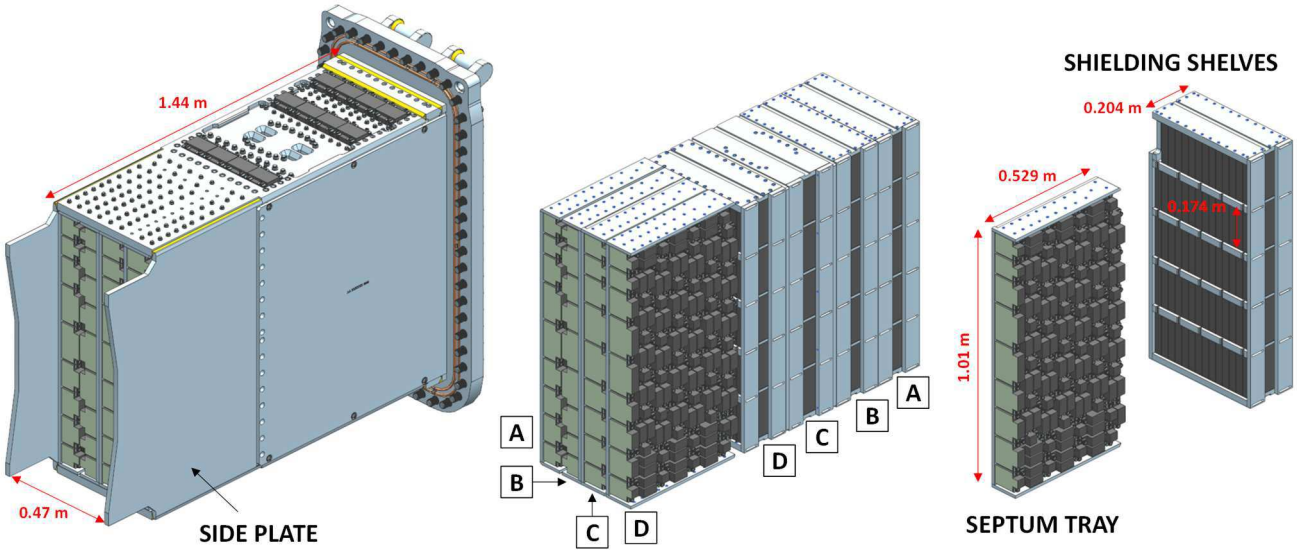

plug flange boundary or radially outward. Re-entrant windows are not allowed due to maintainability.

The main environmental challenges that in-vessel diagnostic sensors face are high temperatures from flash-heating from disruptions, bake, movement of port plugs during poloidal coil energization, and electromagnetic loads from major disruptions. While the plasma facing end of the port plug will heat to 350 degC during a bake through radiation, the air-side of the flange is maintained via resistive heaters to be at 200 degC, which eases integration of windows and feedthroughs. The flash heating from short, $\Delta t_{TQ} < 1\,ms$, thermal quench, mitigated disruptions is a credible risk for components near the front of the port, if left unshielded. The design approach is not to eliminate the risk of flash melting of steel, but to ensure that if it were to occur

Figure VI. Layout and sizing of a fully-shielded off-midplane port plug for SPARC. Lower and upper off-midplane port plugs are interchangeable.

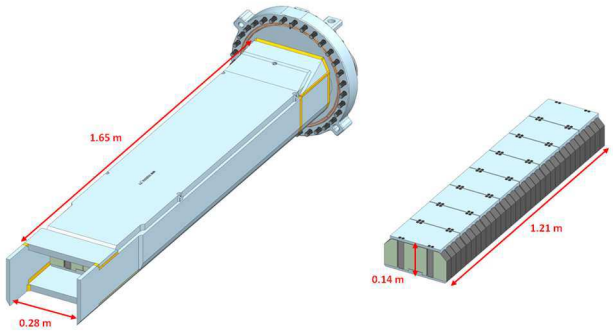

that any functional component of the diagnostic is shielded by a component that can tolerate the limited melt. One of the early operational challenges of SPARC is to optimize the disruption prediction, avoidance and mitigation, and the BOLO system incorporates dedicated 3D radiation characterization channels to be used to tune gas fill and timing of the six toroidally and poloidally space massive gas injection valves, shown as DMS in Figure IV.

The out-of-plane force generated by the TF and PF coil interaction and the up/down asymmetries in the load-path from the port-plugs to the facility result in small motion of the port plugs relative to Tokamak Hall components. Details are outside the focus of this manuscript, but the net impact is to have positions on the port-plugs move ~2 mm between the start of pulse to start of flattop. For some diagnostics this creates ignorable, minor change in observed field of view, but for long-path length optical systems this needs to be accounted for in sizing of in-vessel components and real-time control of ex-vessel relay optics. Pointing of lasers and distortion of light collection optics mounted in the septum trays and shielding shelves use port plug displacements when finalizing components.

The MD scenario described in Section II is the main structural design driver for diagnostics in both the midplane and off-midplane port plugs. Disruption induced bending stresses and toroidal flowing currents that drive the design in in-vessel components are less in magnitude in the port-plugs. This, the lower local dB_p/dt and lower B_t by $\sim 1/R$, allows diagnostic components in the port plugs to grow in size when compared to what can fit below the PFCs. The cantilevered design of the port plugs adds an additional 6.7

g and 10.0 g vertical acceleration for the midplane and off-midplane ports, respectively. It is possible to expose port-plug mounted components to halo currents if features are far forward on the side plate, resulting in a JxB shear force, but this is very application specific. Overall, sustained design iterations across a wide range of diagnostic sub-systems have resulted in rough finding that structures with linear dimensions above the 200-300 mm range end up being beyond stress allowables.

In contrast to in-vessel diagnostics, it is expected that the SPARC port-based diagnostics will be replaced over time with new and further optimized tools. SPARC presently has no material exchange capability (e.g. DIMES [25]) or scanning Langmuir probes [26] due to the engineering risk they pose in a high-field, D-T environment. Once SPARC operates and uncertainties in the disruption loads are reduced, these standard investigatory tools could be integrated. For similar reasons, for the first generation of port-plugs, SPARC has chosen to not include shutters to cover in-vessel optics. Plasma viewing optics have been collimated and moved radially away from the plasma as much as feasible.

VI. DIAGNOSTIC LABS

Utilization of the Diagnostic Labs is expected to be open to CFS-funded collaborators or other research teams that contribute equipment through in-kind contributions [3]. This makes safety an important consideration, and system layout and design have worked to minimize the risk of tritium exposure in the labs. The VCSP spectrometer [22], which must share the vacuum environment with the tokamak, is fully contained in the Tokamak Hall. The XRAY beamlines [23] are mechanically continuous through the east wall, but their vacuum environment is isolated from the tokamak with a double-window, He-backfilled interspace. The vacuum vessel reference ground is brought into the Diagnostic Labs for multiple in-vessel diagnostics. This leads to an electrical hazard which results in the Diagnostic Labs not being able to be occupied during even a H_2 SPARC pulse. Design of the shielding blocks to replace the voids shown in Figure II are ongoing. Similar to port-plugs, 'dog-legs' are utilized for as many systems as possible and straight through penetrations are minimized in diameter. For both XRAY and neutron diagnostics (NTRN), direct line of sight is required, and beam stops in the Diagnostic Labs of 1.0-1.5 m have been estimated.

The Lab spaces have basic power and plant services routed to them to support a wide range of diagnostics. Presently they share up to 240 kW of power, and the waste heat can be removed by chilled water (~200 kW) and HVAC. The Lab spaces are temperature controlled between 70-72 degF with a maximum relatively humidity of 55%. The Tokamak Hall is maintained at a slightly negative pressure relative to the Diagnostic Labs, for the purposes of maintaining a known air flow pattern. Gas and compressed air are available to the Labs, but there are no cryogenic feeds, with LN_2 available on-site through manual fill and hand-carry. Data systems are presently scoped to handle independent 100 Gb/s links to each of the Diagnostic Labs. Details of SPARC data storage and management of diagnostic data will be the focus of future publications.

A key feature of SPARC is being able to operate in D-T and a priority of the early campaign diagnostics is to measure $Q_{fus} > 1$. Section II, IV and V have limited mention of neutron diagnostics. This is due to the decoupling between some of the largest design challenges and features of SPARC with those that drive neutron diagnostic design. An overview of the NTRN system is provided in [27], but the important enabling features are the B4C shielding layout in the 0-DEG port opening and the Diagnostic Lab space behind the NC0-NC6 penetrations in the east wall. The 0-DEG port opening in the vacuum vessel is not occupied by a port-plug, but by VV-mounted shielding, adapting design concepts from the septum trays. Also at 0-DEG is where the torus is pumped, which benefits from having as large an opening in the shielding as possible. The shielding has thus been arranged to effectively create a limiting aperture in the 0-DEG port, which enables the tokamak to be used as a pinhole imaging camera to map the neutron emission image onto the east wall vertically over the NC0 slot. This creates a local zone of high directed neutron flux, ~5e11 n/cm^2/s vs. the typical, more isotropic and lower energy flux of ~1e11 n/cm^2/s , that can be sampled by a variety of NTRN diagnostics, simultaneously. Toroidally and poloidally away from the 0-DEG midplane port, SPARC is as heavily shielded as possible to avoid overheating magnets. This results in a D-T neutron monitoring approach which must evolve from concepts developed at JET and TFTR where the nominally toroidally uniform emission source from the plasma was also observable in the Tokamak Hall. SPARC, in essence, has selectively punctured its B_4C 'blanket' to enable a stream of neutrons to feed diagnostics in a dedicated zone around the central Diagnostic Lab.

XI. SUMMARY

Commonwealth Fusion Systems is leading the design and construction of the compact, high-field SPARC tokamak to extend the physics basis for tokamaks and demonstrate a pathway to commercial fusion energy on a timescale that can impact climate change. To achieve these goals in a timely manner, SPARC must be equipped for its early campaigns with sufficient plasma diagnostics to support operations and gain important scientific insights from new regimes. This manuscript outlines the major design drivers ranging from facility-level down to vacuum-vessel and port-plug level. The layout and description of planned diagnostics and their performance function are provided,

with the intent on references included here and future publications citing this manuscript as holding the detailed quantitative performance requirements. Details of the vacuum vessel and port-plug integration environment are provided along with features of the Diagnostic Labs. Sufficient detail is given within this manuscript to allow for those interested in scoping for future SPARC diagnostics to independently be able to reach early conceptual evaluation.

XII. ACKNOWLEDGMENTS

This work supported by Commonwealth Fusion Systems. Thanks to the broader team that supports the work of the SPARC Diagnostics systems. The authors would also like to acknowledge the dozens of experts from institutions around the world who have contributed by being external reviewers on design reviews for the SPARC diagnostics.

XIII. AUTHOR DECLARATIONS

A. Conflict of interest statement

All authors are financially supported by Commonwealth Fusion Systems either as employees or through sponsored research contracts. CFS is seeking to commercialize fusion energy and may benefit financially from the science and technologies discussed in this manuscript.

B. Ethics approval statement

Not applicable to this manuscript

C. Author contributions

To be filled out for final submission to RSI

XIV. DATA AVAILABILITY STATEMENT

The data the support the findings of this study are available from the corresponding author upon reasonable request.

XV. REFERENCES AND FOOTNOTES

[1] D.G Whyte, *et al*. IEEE Trans. On Appl. Supercond. **34** (2024)
[2] M. Greenwald, *et al*. Phys. Plasmas **21** 110501 (2014)
[3] A.J. Creely, *et al*. Phys. Plasmas. **30** 090601 (2023)
[4] B.N. Sorbom, *et al*. Fusion Eng. Des. **100** 378 (2015)
[5] A.Q. Kuang, *et al*. Fusion Eng. Des. **137** 221 (2018)
[6] T. Golfinopolous, *et al*. IEEE Trans. On Appl. Supercon. **34** (2024)
[7] K. Young Fus. Sci. Tech. **53** 281 (2008)
[8] W. Biel, *et al*. Fusion Eng. Des. **146** 465 (2019)
[9] P. Rodriquez-Fernandez, *et al*. "Core performance prediction in project SPARC first-campaign plasmas with nonlinear CGRYO" submitted to Phys. Plasmas (2024)
[10] Y.K. Oh, *et al*. Fus. Eng Des. **84** 344 (2009)
[11] See https://github.com/cfs-energy/
[12] T. Looby, *et al*. Fus. Sci. Tech. **78** 10 (2022)
[13] I. Zatz, *et al*. IEEE/NPSS Symposium Fusion Engineering **2** 699 (1993)
[14] N.W. Eidietis, *et al*. Nucl. Fusion **55** 063030 (2015)
[15] I.G. Stewart, *et al*. Nucl. Fusion **63** 126014 (2023)
[16] E. Fox-Widdows, these proceedings
[17] R. Li, these proceedings
[18] M. Hanson, these proceedings
[19] A.Q. Kuang, *et al*. J. Plasma Phys. **86** 865860505 (2020)
[20] C. Cowley, *at al*. Plasma Phys. Control. Fusion **65** 035011
[21] J. Hawke, these proceedings
[22] D. Vezinet, these proceedings
[23] I. Song, these proceedings
[24] V. Nikolaeva, these proceedings
[25] C.P.C. Wong, *et al*. J. Nucl. Mater. **196-198** 871 (1992)
[26] D. Brunner, *et al*. Rev. Sci. Instrum. **88** 073501 (2017)
[27] P. Raj, these proceedings